Original Article | Thoracic Imaging

eISSN 2005-8330
https://doi.org/10.3348/kjr.2019.0936
Korean J Radiol 2020;21(9):1104-1113

Korean Journal of Radiology
KJR

Visual and Quantitative Assessments of Regional Xenon-Ventilation Using Dual-Energy CT in Asthma-Chronic Obstructive Pulmonary Disease Overlap Syndrome: A Comparison with Chronic Obstructive Pulmonary Disease

Hye Jeon Hwang, MD, PhD[1], Sang Min Lee, MD, PhD[1], Joon Beom Seo, MD, PhD[1], Jae Seung Lee, MD, PhD[2], Namkug Kim, PhD[1], Sei Won Lee, MD, PhD[2], Yeon-Mok Oh, MD, PhD[2]

[1]Department of Radiology and Research Institute of Radiology, Asan Medical Center, University of Ulsan College of Medicine, Seoul, Korea; [2]Department of Pulmonary and Critical Care Medicine, and Clinical Research Center for Chronic Obstructive Airway Diseases, Asan Medical Center, University of Ulsan College of Medicine, Seoul, Korea

Objective: To assess the regional ventilation in patients with asthma-chronic obstructive pulmonary disease (COPD) overlap syndrome (ACOS) using xenon-ventilation dual-energy CT (DECT), and to compare it to that in patients with COPD.
Materials and Methods: Twenty-one patients with ACOS and 46 patients with COPD underwent xenon-ventilation DECT. The ventilation abnormalities were visually determined to be 1) peripheral wedge/diffuse defect, 2) diffuse heterogeneous defect, 3) lobar/segmental/subsegmental defect, and 4) no defect on xenon-ventilation maps. Emphysema index (EI), airway wall thickness (Pi10), and mean ventilation values in the whole lung, peripheral lung, and central lung areas were quantified and compared between the two groups using the Student's *t* test.
Results: Most patients with ACOS showed the peripheral wedge/diffuse defect (n = 14, 66.7%), whereas patients with COPD commonly showed the diffuse heterogeneous defect and lobar/segmental/subsegmental defect (n = 21, 45.7% and n = 20, 43.5%, respectively). The prevalence of ventilation defect patterns showed significant intergroup differences ($p < 0.001$). The quantified ventilation values in the peripheral lung areas were significantly lower in patients with ACOS than in patients with COPD ($p = 0.045$). The quantified Pi10 was significantly higher in patients with ACOS than in patients with COPD ($p = 0.041$); however, EI was not significantly different between the two groups.
Conclusion: The ventilation abnormalities on the visual and quantitative assessments of xenon-ventilation DECT differed between patients with ACOS and patients with COPD. Xenon-ventilation DECT may demonstrate the different physiologic changes of pulmonary ventilation in patients with ACOS and COPD.
Keywords: *Asthma-chronic obstructive pulmonary disease overlap syndrome; Chronic obstructive pulmonary disease; Dual-energy computed tomography; Ventilation; Xenon*

INTRODUCTION

Chronic obstructive pulmonary disease (COPD) and asthma are considered distinct diseases. However, they share similar physiologic and clinical features, and they are considered as heterogeneous diseases that often have

Received: December 12, 2019 **Revised:** March 11, 2020 **Accepted:** March 22, 2020
This study was funded by Bracco Imaging Korea, Seoul, South Korea.
Corresponding author: Sang Min Lee, MD, PhD, Department of Radiology and Research Institute of Radiology, University of Ulsan College of Medicine, Asan Medical Center, 88 Olympic-ro 43-gil, Songpa-gu, Seoul 05505, Korea.
• E-mail: asellion@hanmail.net

Korean Journal of Radiology
KJR

overlapping conditions (1-3). Recently, the Global Initiative for Asthma and the Global Initiative for Chronic Obstructive Lung Disease guidelines accepted the concept of asthma-COPD overlap syndrome (ACOS), which is characterized by persistent airflow limitation with several features usually associated with asthma and COPD alone (4). Previous studies have compared the characteristics between patients with ACOS and those with asthma or COPD alone, and have reported that patients with ACOS have more rapid declines in lung function, more frequent exacerbations, higher mortality rates, and greater need for medical resources (1, 5-8). Patients with ACOS may require distinct clinical evaluation and treatment, and their proper management may require an understanding of the pathophysiology of ACOS.

CT is widely used for assessing pulmonary abnormalities in patients with COPD and asthma, and quantitative CT analysis provides objective information about pulmonary parenchymal changes (9-12). Moreover, dual-energy CT (DECT) with xenon-ventilation imaging, which can provide high-resolution anatomic information and pulmonary ventilation status concurrently with single CT scanning, has been used to investigate regional ventilation changes in patients with various obstructive lung diseases including asthma and COPD (13-16). However, no studies have reported the use of DECT or other imaging modalities to assess the parenchymal ventilation changes in patients with ACOS. Therefore, we aimed to assess the regional ventilation status in patients with ACOS by using xenon-ventilation DECT and to compare it to that of patients with COPD.

MATERIALS AND METHODS

Patients

This prospective study was approved by our Institutional Review Board. Written informed consent was obtained after the explanation of the study and the disclosure of the patients' clinical information. Between May 2012 and December 2016, we recruited 21 patients with ACOS and 46 patients with COPD from our pulmonology clinic. The diagnoses of ACOS and COPD were made by a pulmonologist according to the joint statement released by the Global Initiative for Asthma and the Global Initiative for Chronic Obstructive Lung Disease (4). Among these patients, 27 patients with COPD were included in the previous study (15). All patients underwent xenon-ventilation DECT, pulmonary function test (PFT) with a spirometer, diffusion capacity measurement, and the 6-minute walk distance test (6MWT) on the same day.

Xenon-Ventilation DECT and Postprocessing

Patients inhaled 30% stable xenon gas using a face mask designed for positive pressure ventilation treatments (King Systems Corporation, Noblesville, IN, USA) and a xenon gas inhalation system (Zetron V, Anzai Medical, Tokyo, Japan). We monitored xenon concentration in the inhaled and exhaled gases throughout the study. After the xenon concentration in the exhaled gas reached 25%, a full-thoracic CT was performed using the SOMATOM Flash CT (Siemens Healthineers, Forchheim, Germany) (55/130 eff. mA at sn140/80 kV, 64 x 0.6 mm collimation, 0.55 pitch, and 0.2-second rotation time) (15). A detailed description about CT protocol can be found in the Supplementary Materials.

In postprocessing, virtual non-contrast (VNC) images and xenon-ventilation maps were obtained from the 80- and Sn140-kV images using the modified "liver VNC" and "xenon" applications of Syngo Dual Energy (Siemens Healthineers). Image data were reconstructed with a 1.5-mm section thickness using kernel D30 at 1.5-mm increments.

Visual Analysis of Xenon-Ventilation Patterns

Xenon-ventilation in the lung parenchyma was displayed on the color-coded xenon-ventilation maps by using the xenon-attenuation value. The two axial image sets (VNC image and xenon-ventilation map) were simultaneously displayed using in-house software. The presence of ventilation defects was judged based on the normal lung findings on the xenon-ventilation maps from a previous study (13). Areas enhanced by xenon were displayed as orange, yellow, and green, and were interpreted as showing normal ventilation. Areas with poor or no enhancement by xenon were displayed as blue or purple on our xenon-ventilation maps (Fig. 1). Blue-to-purple-colored areas, which were sharply demarcated from normal yellow-to-green areas, indicated ventilation defects. Two chest radiologists (with 11 and 9 years of experience in thoracic radiology, respectively), blinded to the diagnosis of cases, determined the xenon-ventilation abnormality patterns in consensus to represent 1) peripheral wedge/diffuse defects (ventilation defects not extending to the hilum or central lung areas), 2) diffuse heterogeneous defects (ventilation defects and normal ventilation areas intermixed throughout the lungs), 3) lobar/segmental/subsegmental defects (ventilation

 https://doi.org/10.3348/kjr.2019.0936

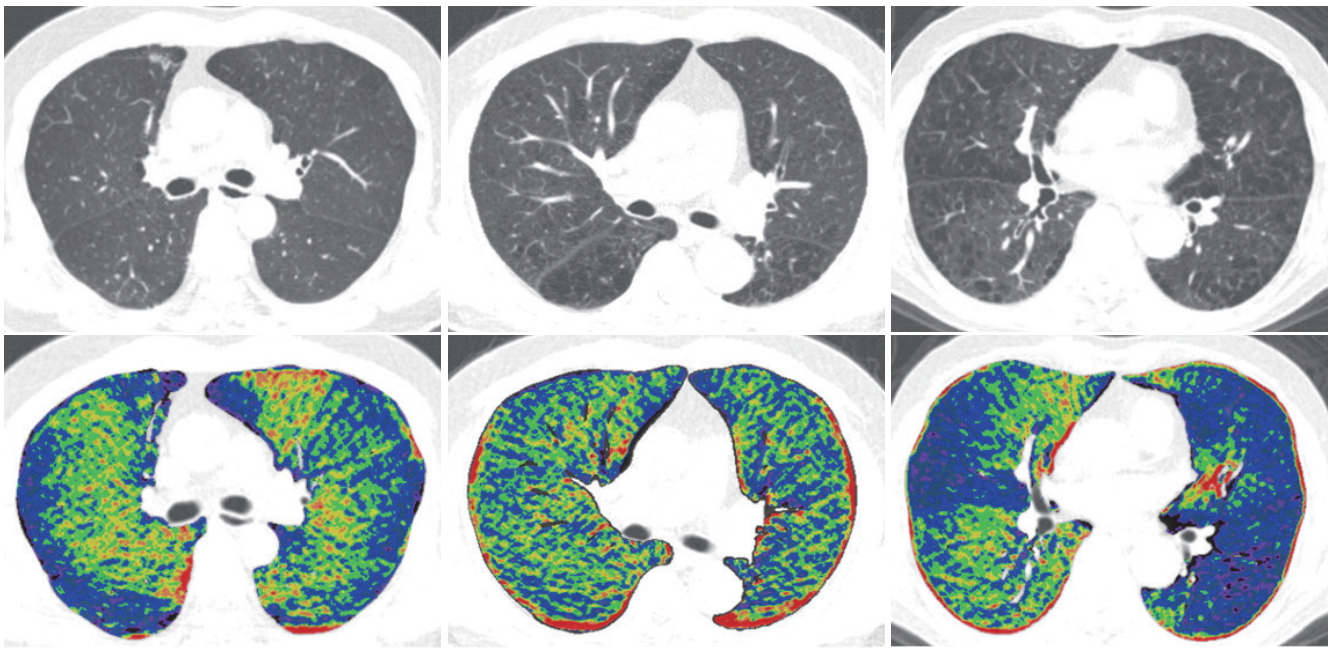

Fig. 1. Ventilation defect patterns on xenon-ventilation maps for visual analysis of ventilation abnormalities.
A. Peripheral wedge/diffuse defect pattern shows xenon-enhancement defect in peripheral half from pleural surface of lung. Ventilation defects do not extend to hilum or central lung areas. **B.** Diffuse heterogeneous defect pattern shows uneven mixture of small areas with normal ventilation and poor ventilation throughout lung. **C.** Lobar/segmental/subsegmental defect shows segmental or lobar distribution of ventilation defects extending to hilum or central lung area.

defects extending to the hilum or central lung area with lobar, segmental, or subsegmental distribution), and 4) no defects (Fig. 1). We categorized these patterns according to the descriptions in the previous studies (13-15, 17, 18). If one patient had any two or three intermixed ventilation patterns, the most predominant pattern was used to describe the abnormality. Areas of parenchymal abnormality on VNC images, possibly showing ventilation abnormalities such as atelectasis or sequelae, were excluded during the visual assessment of ventilation defects. The highest and lowest ventilation values in the regions at the thoracic wall (dorsal part) and around the heart were thought to have been caused by the inherent artifacts from the current dual-source DECT acquisition, including offset of acquisition between two different X-ray tubes and beam-hardening artifact. We excluded such regions from the visual analysis.

Quantitative Analysis of Ventilation and Quantitative CT Densitometry

Ventilation values on xenon-ventilation DECT were quantified using in-house software. After the automatic extraction of the whole lung, the ventilation values, i.e., the mean Hounsfield unit (HU) of the xenon map in the lung parenchyma, of the whole lung area were quantified. The whole lung was divided into the peripheral and central lungs using theoretical lung surface lines drawn at 20-mm depths from the lung surface (19). Thereafter, the ventilation values in the peripheral and central lung areas were quantified. The emphysema index (EI; the percentage of the area below -950 HU in the lung parenchyma) (20-22) and airway measurement were determined using commercial software (Aview, Coreline Soft, Seoul, Korea) on VNC images. For airway measurement, Pi10, which is the square root of the wall area of the theoretical airway with a 10-mm internal perimeter (23), was obtained using the integral-based half-band algorithm (24). We obtained the Pi10 value by creating regression plots of the square root of the wall area against the corresponding internal perimeter of the 5th–8th branches of the airways in all segments of both lungs (25).

Statistical Analysis

Baseline characteristics, PFT and 6MWT results, and quantified CT parameters were compared between the ACOS and COPD groups by using Student's *t* test. The prevalence of ventilation abnormality patterns was compared between the groups by using the χ^2 test. Pearson's correlation analysis was used to compare the quantified CT values and PFT results. All statistical analyses were performed

https://doi.org/10.3348/kjr.2019.0936

Korean Journal of Radiology
KJR

using SPSS version 21.0 (IBM Corp., Armonk, NY, USA). The quantified variables are expressed as means ± standard deviation. $P < 0.05$ indicated statistical significance.

RESULTS

Patients' Characteristics

The patients' clinical characteristics are summarized in Table 1. No significant intergroup differences were observed in age, body mass index, smoking history, and PFT and 6MWT results, except for the carbon monoxide diffusing capacity corrected for hemoglobin concentration (DL_{CO}), which was significantly higher in the ACOS group than in the COPD group.

Visual Analysis of Xenon-Ventilation Patterns

On visual analysis, all patients showed morphologic abnormalities such as emphysema, bronchial wall thickening, or parenchymal air trapping on VNC images. The CT findings on VNC images were visually indistinguishable between the ACOS and COPD groups.

All patients in the ACOS and COPD groups showed diffuse or regional ventilation abnormalities on the xenon-ventilation maps. Ventilation abnormalities in patients with ACOS most often appeared as peripheral wedge/diffuse defects (14/21, 66.7%), which were seen mostly in the periphery of the middle-to-lower lung areas and had a wedge-shaped or diffuse configuration (Figs. 1, 2). In this pattern, the ventilation defects were confined to the peripheral half or one-third of the pleural surface of the lung parenchyma. The boundaries of most ventilation defects were well demarcated from the surrounding normally ventilated lung. The areas without ventilation defects mostly showed homogeneous xenon enhancement in patients with ACOS. In patients with COPD, peripheral wedge/diffuse defects were only seen in 5 of 46 (10.9%), and diffuse heterogeneous defects (21/46, 45.7%) were the most common, followed by lobar/segmental/subsegmental defects (20/46, 43.5%). In the diffuse heterogeneous defect pattern, ventilation defects were seen throughout the lung, with a mixture of small areas with normal and poor ventilation. Lobar/segmental/subsegmental defects in patients with COPD mostly involved one segment and extended into the central half of the lung. In some patients with COPD, both diffuse heterogeneous defects and lobar/segmental/subsegmental defects were seen concurrently. The prevalence of the three patterns showed significant intergroup differences ($p < 0.001$) (Table 2).

Quantitative Analysis of Xenon-Ventilation and Quantitative CT Densitometry

The quantified ventilation value of the peripheral lung area was significantly lower in the ACOS group than in the COPD group ($p = 0.045$); however, the values of the whole and central lung areas showed no significant intergroup differences (Table 3). The mean EI values of the whole lung

Table 1. Demographic Information and Pulmonary Function Test Results in ACOS and COPD Groups

Variables	ACOS (n = 21)	COPD (n = 46)	P*
Age (years)	66.1 ± 7.6	67.4 ± 7.2	0.504
Sex (n)	M:F = 20:1	M:F = 46:0	N/A
Body mass index (kg/m^2)	24.4 ± 2.9	23.8 ± 3.0	0.482
Smoking history (pack-years)	43.1 ± 25.2	41.5 ± 13.4	0.729
FEV_1 (%pred)	54.8 ± 11.0	55.1 ± 14.1	0.932
FVC (%pred)	85.5 ± 10.8	84.2 ± 12.7	0.700
FEV_1/FVC (%)	45.8 ± 8.8	46.7 ± 11.9	0.750
DL_{CO} (corrected %pred)	74.0 ± 12.6	64.2 ± 19.7	0.042†
TLC (%pred)	101.4 ± 11.3	95.9 ± 13.8	0.119
VC (%pred)	98.2 ± 12.9	96.4 ± 14.4	0.627
FRC (%pred)	119.3 ± 22.5	118.6 ± 26.6	0.915
RV (%pred)	106.7 ± 29.9	96.4 ± 32.7	0.226
6MWT (m)	480.6 ± 66.4	465.9 ± 79.8	0.465

Values are expressed as means ± standard deviation. 6MWT data are available for 45 patients. *Comparison between ACOS and COPD groups is performed using Student's *t* test, †Value is statistically significant ($p < 0.05$). ACOS = asthma-COPD overlap syndrome, COPD = chronic obstructive pulmonary disease, DL_{CO} = carbon monoxide diffusing capacity corrected for hemoglobin concentration, FEV_1 = forced expiratory volume in 1 second, FRC = functional residual capacity, FVC = forced vital capacity, m = meter, NA = not applicable, RV = residual volume, TLC = total lung capacity, VC = vital capacity, 6MWT = 6-minute walk distance test, %pred = percentage predicted value

https://doi.org/10.3348/kjr.2019.0936

were 7.7 ± 6.6% in the ACOS group and 12.0 ± 12.4% in the COPD group. The EI showed no significant intergroup differences (p = 0.070); however, the ACOS group showed a tendency towards a lower EI than did the COPD group. The average Pi10 measurements in the ACOS and COPD groups were 5.04 ± 0.55 and 4.66 ± 0.72, respectively; the segmental airways were thicker in the ACOS group than in the COPD group (p = 0.041).

Correlation between Quantified CT Parameters and PFT Results

The ventilation value of the central lung area showed a significant positive correlation with the forced expiratory volume in 1 second (FEV_1) in patients with ACOS (r = 0.499, p = 0.025). The value of the whole lung area also showed a tendency towards a positive correlation with FEV_1; however,

Table 2. Visual Analysis of Ventilation Defect Patterns in Patients with ACOS and COPD

Disease	Pattern (1)	Pattern (2)	Pattern (3)	P*
ACOS (n = 21)	14 (66.7)	2 (9.5)	5 (23.8)	< 0.001†
COPD (n = 46)	5 (10.9)	21 (45.7)	20 (43.5)	

Data are numbers of patients with percentages in parentheses. *Comparison between ACOS and COPD groups is performed using χ^2 test, †Value is statistically significant (p < 0.05). Pattern (1), peripheral wedge/diffuse defect; Pattern (2), diffuse heterogeneous defect; Pattern (3), lobar/segmental/subsegmental defect.

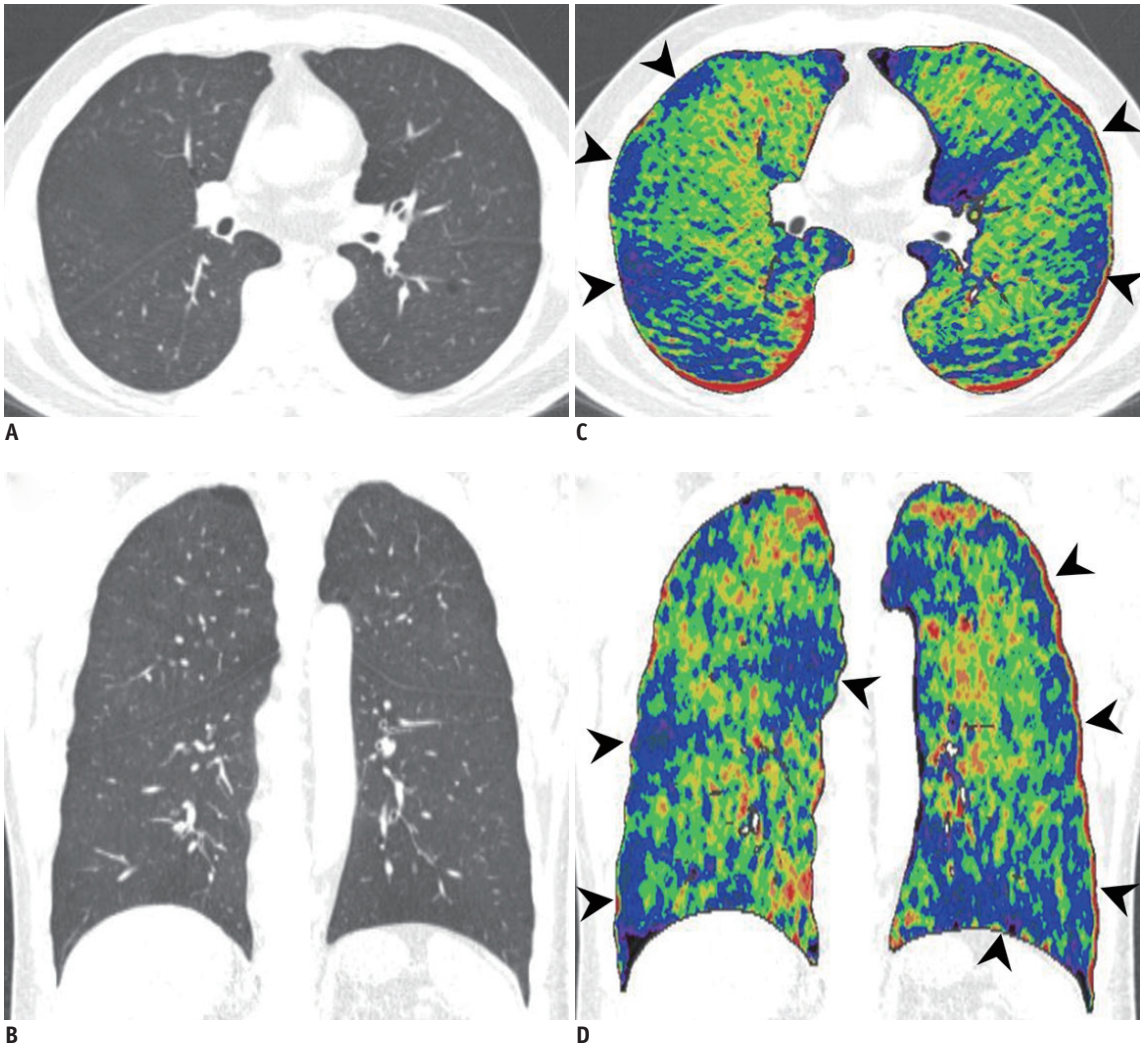

Fig. 2. Peripheral wedge/diffuse defect pattern of xenon-ventilation in 54-year-old man with ACOS (emphysema index = 5.73, square root of wall area of airway with 10-mm internal perimeter = 5.42).
A, B. Axial and coronal weighted average images of dual-energy CT show diffuse bronchial wall thickening with minimal centrilobular emphysema. **C, D.** Axial and coronal xenon-ventilation maps show multifocal wedge-shaped or patchy areas showing blue-to-purple color in peripheral lung areas, indicating ventilation defects (arrowheads). We considered linear or ovoid or patchy-shaped black-, purple-, blue-, or red-colored areas around vertebral body, heart, and dorsal part of lung on xenon map as artifacts. We excluded these areas from visual analysis. ACOS = asthma-chronic obstructive pulmonary disease overlap syndrome

https://doi.org/10.3348/kjr.2019.0936

Korean Journal of Radiology
KJR

Table 3. Quantitative Analysis of Xenon-Ventilation and Quantitative CT Densitometry in Patients with ACOS and COPD

Variables	ACOS	COPD	*P**
Emphysema index (%)	7.7 ± 6.6	12.0 ± 12.4	0.070
Airway measurement (Pi10) (mm)	5.0 ± 0.6	4.7 ± 0.7	0.041†
Ventilation_whole lung (HU)	22.2 ± 2.2	23.3 ± 3.7	0.130
Ventilation_peripheral lung (HU)	21.3 ± 2.3	22.8 ± 3.7	0.045†
Ventilation_central lung (HU)	24.1 ± 2.4	24.4 ± 4.1	0.710

Values are expressed as means ± standard deviation. *Comparison between ACOS and COPD groups is performed using Student's *t* test, †Value is statistically significant ($p < 0.05$). HU = Hounsfield unit, Pi10 = square root of wall area of airway with 10-mm internal perimeter

it was not statistically significant ($r = 0.286$, $p = 0.222$) (Fig. 3A, B, Supplementary Table 1). The value of the peripheral lung area was not significantly correlated with FEV_1. The EI showed negative correlations with FEV_1/forced vital capacity (FVC) and DL_{CO} ($r = -0.510$, $p = 0.018$ and $r = -0.445$, $p = 0.043$, respectively) in patients with ACOS. The EI also showed a tendency towards a negative correlation with FEV_1; however, it was not statistically significant ($r = -0.310$, $p = 0.171$) in the ACOS group. In patients with COPD, the EI showed significant negative correlations with FEV_1, FEV_1/FVC, DL_{CO}, and 6MWT results, and the ventilation values of the whole, central, and peripheral lung areas showed significant positive correlations with most of the PFT results (Fig. 3C, D, Supplementary Table 2).

DISCUSSION

Our study showed that the xenon-ventilation DECT may demonstrate different ventilation abnormalities predominantly seen in patients with ACOS or COPD. Fourteen of 21 patients with ACOS showed the wedge/diffuse ventilation defects in the periphery of the mid-to-lower lungs. However, most patients with COPD showed diffuse heterogeneous defects throughout the lung or lobar/segmental/subsegmental defects. The quantified xenon-ventilation value of the peripheral lung areas was also significantly lower in patients with ACOS than in patients with COPD. The values of the whole and central lung areas showed a tendency towards a positive correlation with FEV_1, with the central lung values showing statistical significance.

Parenchymal ventilation abnormalities in the obstructive lung diseases have been investigated using various imaging modalities, such as magnetic resonance imaging (MRI), single-photon emission computed tomography, and DECT (13, 14, 26-32). Although static anatomic imaging is dominant in clinical practice, the functional imaging evaluating parenchymal ventilation may enhance our understanding of physiologic changes or structural-functional relationships in the obstructive lung diseases, as well as physiologic changes after treatments (33). DECT has advantages in providing both high-resolution anatomic information and functional information with single CT scanning. To our knowledge, the ventilation abnormalities in patients with ACOS have not been documented at a morphologic level, and we investigated the ventilation abnormalities in patients with ACOS by using xenon-ventilation DECT and compared them to those in patients with COPD. Although patients with ACOS and COPD could not be discriminated using VNC images, patients with ACOS mostly showed the peripheral wedge/diffuse ventilation defects on xenon-ventilation maps, unlike patients with COPD.

The predominant ventilation defect patterns in each group differed in our study, even though both groups shared some ventilation defect patterns on xenon-ventilation DECT. The precise pathophysiology of ventilation defects on various ventilation imaging remains unclear, and the authors of the previous studies explained and estimated the causes of ventilation defect patterns according to the pathophysiologic characteristics of each disease. The peripheral wedge ventilation defect is frequently seen on various ventilation images performed in asthmatics (14, 34). Since asthma is characterized by mucus hypersecretion, airway hyperreactivity, and airway edema, it seems likely that the cause of the peripheral wedge ventilation defects in asthmatics is small airway obstruction from some combination of these factors (34, 35). In these subjects, the ventilation defects also reversed following bronchodilator inhalation, and this reversal is likely due to dilation of the small airways, allowing air to pass through previously constricted airways (16, 35). The heterogeneous or patchy or lobar/segmental/subsegmental defects have been reported in the COPD group (13, 15), and these patterns may be seen in one patient at the same

 https://doi.org/10.3348/kjr.2019.0936

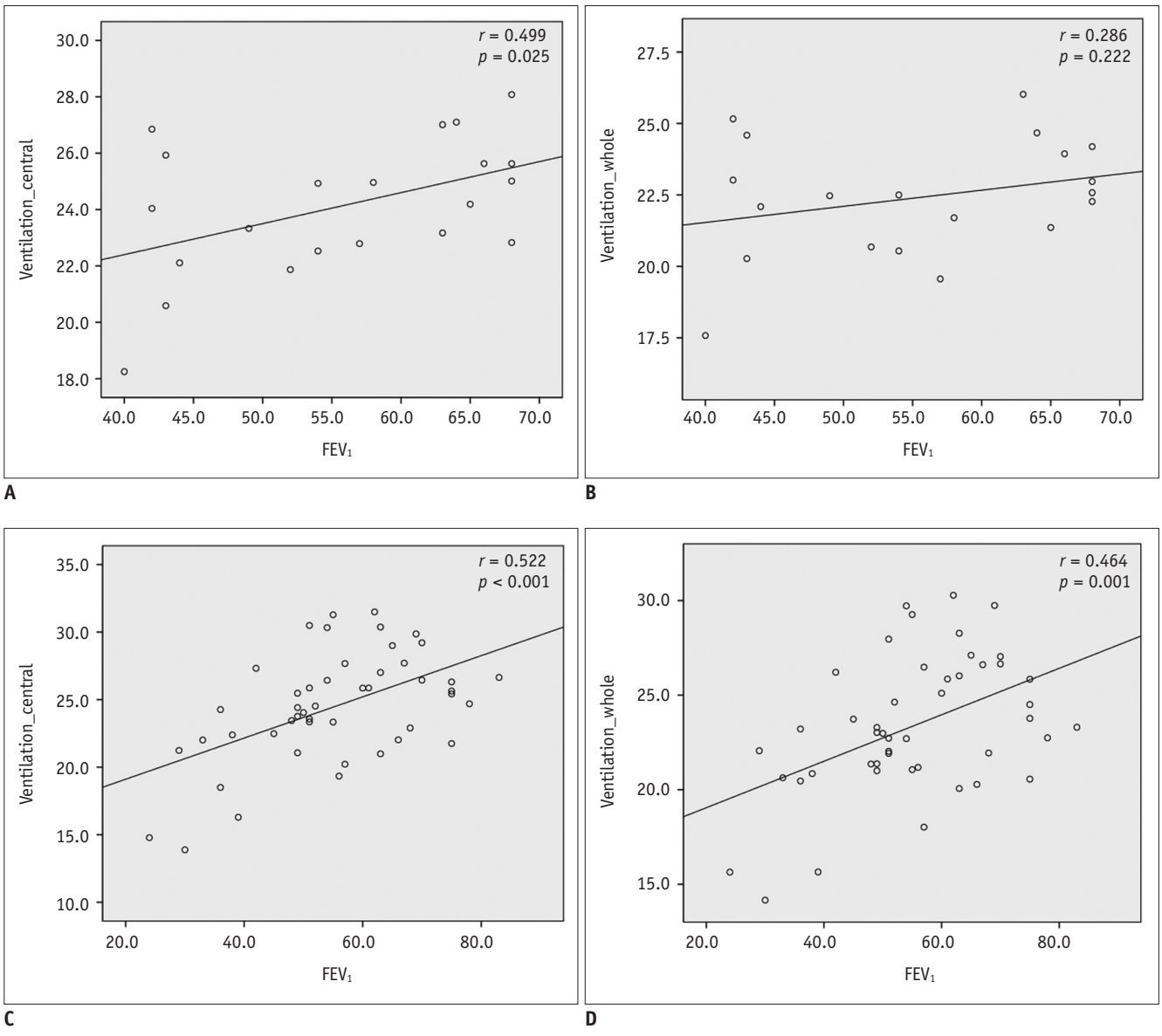

Fig. 3. Results of correlation analysis of quantified xenon-ventilation values and FEV_1.
A. Xenon-ventilation values of central lung area show significant positive correlation with FEV_1. **B.** Xenon-ventilation values of whole lung area show tendency towards positive correlation with FEV_1 in patients with ACOS. **C, D.** Xenon-ventilation values of both central and whole lung areas show significant positive correlations with FEV_1 in patients with chronic obstructive pulmonary disease. FEV_1 = forced expiratory volume in 1 second

time. COPD is characterized by a loss of parenchymal recoil, and thus hyperinflation, peripheral airway obstruction, airway inflammation resulting in obstruction of both large and small airways, and various combinations of these factors are thought to be responsible for the ventilation defects in COPD. Since the predominant ventilation defect pattern in the ACOS group was like that in asthmatics, the similar etiology may be associated with the characteristic ventilation defect pattern in the ACOS group. Although the airway disease in ACOS may have the characteristics of both COPD and asthma, the characteristics of small airway disease that may result in ventilation defects in ACOS may be similar to those of asthma.

Our study showed that thicker segmental airways (higher Pi10) are associated with the patients with ACOS, even though our patient groups were matched for their demographic characteristics and baseline PFT characteristics. The emphysema severity showed no intergroup difference; however, the ACOS group showed a tendency towards a lower EI than did the COPD group. These findings are similar

https://doi.org/10.3348/kjr.2019.0936

Korean Journal of Radiology
KJR

to the results of the previous studies (2, 36, 37). Currently, we cannot precisely explain why the thicker segmental airways are seen in the ACOS group compared with the COPD group. However, these results may suggest that ACOS is an airway-dominant disease rather than an emphysema-dominant disease as compared to COPD. Using CT, COPD is characterized as a heterogeneous group that can be divided into emphysema-dominant, airway disease-dominant, or mixed types. Patients with ACOS showed more significant reversibility in the CT-quantified airway wall thickening and air trapping in response to bronchodilator than did patients with COPD in the previous studies (36, 37). These results also suggest that ACOS is a more airway-dominant disease than is COPD. In addition, as we discussed above, the characteristics of airway disease in ACOS may be more like those of asthma than those of COPD. The wall thickness and wall area on CT were greater in asthmatics than in COPD patients in the previous study (38). The relationship between structural and functional airway changes of ACOS patients compared with COPD patients and asthmatics requires further study.

The introduction of ^{129}Xe- or ^{3}He-ventilation MRI and xenon-ventilation DECT has enabled the investigation of ventilation abnormalities in asthma and COPD (13-15, 27, 28, 35, 39, 40). These abnormalities are readily demonstrated as decreased signal intensity on ^{3}He-MRI or ^{129}Xe-MRI, and the number and size or percentage of these abnormalities correlate with disease severity or FEV_1 (27, 28, 35, 40). Xenon-ventilation DECT demonstrates the decreased xenon-enhancement, which can be quantified as the ventilation value. These quantified ventilation values significantly correlated with the clinical parameters of patients with COPD (15, 21); however, they were not significantly correlated with the FEV_1 in asthmatics (41). We quantitatively assessed xenon-ventilation in various lung areas, and it tended to correlate with the PFT results more in patients with COPD than in those with ACOS, despite similar correlation tendencies between the two groups. However, our study was limited by its small number of patients with ACOS; hence, further studies with larger numbers of patients with ACOS are warranted.

Our study has several limitations. First, the ACOS group was relatively small because this was a single-center study. Second, some *p* values (Pi10 and ventilation value in the peripheral lung) of the comparison of CT quantitative values between the ACOS and COPD groups were marginal. However, also in the previous study, ACOS patients had higher wall area percentage (37). Further studies with larger sample sizes are needed for validating this issue. Third, the diagnosis of ACOS was partly based on a retrospective assessment of asthma-related symptoms. Although all our patients with ACOS in this study were diagnosed by an expert pulmonologist, distinguishing ACOS from COPD might be difficult in some patients. Fourth, the consensus visual analysis of xenon-ventilation patterns without validation of the reproducibility or interobserver agreement could be a limitation, although radiologists who experienced in xenon-ventilation image analysis and research performed the visual analyses. Fifth, we used the multiple breath-in method, which might possibly obscure the ventilation defects that can be seen on ^{3}He-MRI using the single breath-in method. However, xenon attenuation with the single breath-in method on DECT was too low; therefore, the multiple breath-in method was required to acquire images with sufficient attenuation for the visual and quantitative analyses. Sixth, we used VNC images to quantify the EI and airway wall thickening. The HU on VNC images may not be identical to that of actual non-contrast CT images. However, a previous study showed a correlation between the quantified parameters of VNC images and PFT results (42).

In conclusion, our study demonstrated the potential of xenon-ventilation DECT, as it shows the different ventilation abnormalities visually and quantitatively in patients with ACOS compared to patients with COPD. Xenon-ventilation DECT can demonstrate different physiologic changes in pulmonary ventilation in patients with ACOS and COPD.

Supplementary Materials

The Data Supplement is available with this article at https://doi.org/10.3348/kjr.2019.0936.

Conflicts of Interest

The authors have no potential conflicts of interest to disclose.

ORCID iDs

Sang Min Lee
https://orcid.org/0000-0002-2173-2193
Hye Jeon Hwang
https://orcid.org/0000-0003-3508-2870
Joon Beom Seo
https://orcid.org/0000-0003-0271-7884

Jae Seung Lee
https://orcid.org/0000-0003-4130-1486
Namkug Kim
https://orcid.org/0000-0002-3438-2217
Sei Won Lee
https://orcid.org/0000-0003-4814-6730
Yeon-Mok Oh
https://orcid.org/0000-0003-0116-4683

REFERENCES

1. Gibson PG, Simpson JL. The overlap syndrome of asthma and COPD: what are its features and how important is it? *Thorax* 2009;64:728-735
2. Hardin M, Cho M, McDonald ML, Beaty T, Ramsdell J, Bhatt S, et al. The clinical and genetic features of COPD-asthma overlap syndrome. *Eur Respir J* 2014;44:341-350
3. Zeki AA, Schivo M, Chan A, Albertson TE, Louie S. The Asthma-COPD overlap syndrome: a common clinical problem in the elderly. *J Allergy (Cairo)* 2011;2011:861926
4. 2015 asthma, COPD and asthma-COPD overlap syndrome (ACOS). Global Initiative for Asthma Web site. https://ginasthma.org/asthma-copd-and-asthma-copd-overlap-syndrome-acos/. Accessed Nov 2, 2017
5. Kauppi P, Kupiainen H, Lindqvist A, Tammilehto L, Kilpeläinen M, Kinnula VL, et al. Overlap syndrome of asthma and COPD predicts low quality of life. *J Asthma* 2011;48:279-285
6. Mannino DM, Gagnon RC, Petty TL, Lydick E. Obstructive lung disease and low lung function in adults in the United States: data from the National Health and Nutrition Examination Survey, 1988-1994. *Arch Intern Med* 2000;160:1683-1689
7. Menezes AMB, Montes de Oca M, Pérez-Padilla R, Nadeau G, Wehrmeister FC, Lopez-Varela MV, et al. Increased risk of exacerbation and hospitalization in subjects with an overlap phenotype: COPD-asthma. *Chest* 2014;145:297-304
8. Rhee CK, Yoon HK, Yoo KH, Kim YS, Lee SW, Park YB, et al. Medical utilization and cost in patients with overlap syndrome of chronic obstructive pulmonary disease and asthma. *COPD* 2014;11:163-170
9. Bakker ME, Putter H, Stolk J, Shaker SB, Piitulainen E, Russi EW, et al. Assessment of regional progression of pulmonary emphysema with CT densitometry. *Chest* 2008;134:931-937
10. Kim SS, Seo JB, Lee HY, Nevrekar DV, Forssen AV, Crapo JD, et al. Chronic obstructive pulmonary disease: lobe-based visual assessment of volumetric CT by using standard images—Comparison with quantitative CT and pulmonary function test in the COPDGene study. *Radiology* 2013;266:626-635
11. Mets OM, Murphy K, Zanen P, Gietema HA, Lammers JW, van Ginneken B, et al. The relationship between lung function impairment and quantitative computed tomography in chronic obstructive pulmonary disease. *Eur Radiol* 2012;22:120-128
12. Park CS, Müller NL, Worthy SA, Kim JS, Awadh N, Fitzgerald M. Airway obstruction in asthmatic and healthy individuals: inspiratory and expiratory thin-section CT findings. *Radiology* 1997;203:361-367
13. Chae EJ, Seo JB, Goo HW, Kim N, Song KS, Lee SD, et al. Xenon ventilation CT with a dual-energy technique of dual-source CT: initial experience. *Radiology* 2008;248:615-624
14. Chae EJ, Seo JB, Lee J, Kim N, Goo HW, Lee HJ, et al. Xenon ventilation imaging using dual-energy computed tomography in asthmatics: initial experience. *Invest Radiol* 2010;45:354-361
15. Hwang HJ, Seo JB, Lee SM, Kim N, Oh SY, Lee JS, et al. Assessment of regional xenon ventilation, perfusion, and ventilation-perfusion mismatch using dual-energy computed tomography in chronic obstructive pulmonary disease patients. *Invest Radiol* 2016;51:306-315
16. Kim WW, Lee CH, Goo JM, Park SJ, Kim JH, Park EA, et al. Xenon-enhanced dual-energy CT of patients with asthma: dynamic ventilation changes after methacholine and salbutamol inhalation. *AJR Am J Roentgenol* 2012;199:975-981
17. King GG, Farrow CE, Chapman DG. Dismantling the pathophysiology of asthma using imaging. *Eur Respir Rev* 2019;28:180111
18. Sugino K, Kobayashi M, Nakamura Y, Gocho K, Ishida F, Isobe K, et al. Xenon-enhanced dual-energy CT imaging in combined pulmonary fibrosis and emphysema. *PLoS One* 2017;12:e0170289
19. Cho YH, Lee SM, Seo JB, Kim N, Bae JP, Lee JS, et al. Quantitative assessment of pulmonary vascular alterations in chronic obstructive lung disease: associations with pulmonary function test and survival in the KOLD cohort. *Eur J Radiol* 2018;108:276-282
20. Bergin C, Müller N, Nichols DM, Lillington G, Hogg JC, Mullen B, et al. The diagnosis of emphysema. A computed tomographic-pathologic correlation. *Am Rev Respir Dis* 1986;133:541-546
21. Lee YK, Oh YM, Lee JH, Kim EK, Lee JH, Kim N, et al. Quantitative assessment of emphysema, air trapping, and airway thickening on computed tomography. *Lung* 2008;186:157-165
22. Nakano Y, Sakai H, Muro S, Hirai T, Oku Y, Nishimura K, et al. Comparison of low attenuation areas on computed tomographic scans between inner and outer segments of the lung in patients with chronic obstructive pulmonary disease: incidence and contribution to lung function. *Thorax* 1999;54:384-389
23. Grydeland TB, Dirksen A, Coxson HO, Pillai SG, Sharma S, Eide GE, et al. Quantitative computed tomography: emphysema and airway wall thickness by sex, age and smoking. *Eur Respir J* 2009;34:858-865
24. Cho YH, Seo JB, Kim N, Lee HJ, Hwang HJ, Kim EY, et al. Comparison of a new integral-based half-band method for CT measurement of peripheral airways in COPD with a conventional full-width half-maximum method using both

https://doi.org/10.3348/kjr.2019.0936

phantom and clinical CT images. *J Comput Assist Tomogr* 2015;39:428-436
25. Park HJ, Lee SM, Choe J, Lee SM, Kim N, Lee JS, et al. Prediction of treatment response in patients with chronic obstructive pulmonary disease by determination of airway dimensions with baseline computed tomography. *Korean J Radiol* 2019;20:304-312
26. Cukic V, Begic A. Potential role of lung ventilation scintigraphy in the assessment of COPD. *Acta Inform Med* 2014;22:170-173
27. de Lange EE, Altes TA, Patrie JT, Battiston JJ, Juersivich AP, Mugler JP 3rd, et al. Changes in regional airflow obstruction over time in the lungs of patients with asthma: evaluation with ^{3}He MR imaging. *Radiology* 2009;250:567-575
28. Kirby M, Mathew L, Wheatley A, Santyr GE, McCormack DG, Parraga G. Chronic obstructive pulmonary disease: longitudinal hyperpolarized ^{3}He MR imaging. *Radiology* 2010;256:280-289
29. Ohno Y, Iwasawa T, Seo JB, Koyama H, Takahashi H, Oh YM, et al. Oxygen-enhanced magnetic resonance imaging versus computed tomography: multicenter study for clinical stage classification of smoking-related chronic obstructive pulmonary disease. *Am J Respir Crit Care Med* 2008;177:1095-1102
30. Stavngaard T, Søgaard LV, Mortensen J, Hanson LG, Schmiedeskamp J, Berthelsen AK, et al. Hyperpolarized ^{3}He MRI and ^{81m}Kr SPECT in chronic obstructive pulmonary disease. *Eur J Nucl Med Mol Imaging* 2005;32:448-457
31. Suga K, Nishigauchi K, Kume N, Koike S, Takano K, Tokuda O, et al. Dynamic pulmonary SPECT of xenon-133 gas washout. *J Nucl Med* 1996;37:807-814
32. Tzeng YS, Hoffman E, Cook-Granroth J, Gereige J, Mansour J, Washko G, et al. Investigation of hyperpolarized ^{3}He magnetic resonance imaging utility in examining human airway diameter behavior in asthma through comparison with high-resolution computed tomography. *Acad Radiol* 2008;15:799-808
33. Lee SW, Lee SM, Shin SY, Park TS, Oh SY, Kim N, et al. Improvement in ventilation-perfusion mismatch after bronchoscopic lung volume reduction: quantitative image analysis. *Radiology* 2017;285:250-260
34. Altes TA, Powers PL, Knight-Scott J, Rakes G, Platts-Mills TA, de Lange EE, et al. Hyperpolarized ^{3}He MR lung ventilation imaging in asthmatics: preliminary findings. *J Magn Reson Imaging* 2001;13:378-384
35. Farah CS, King GG, Brown NJ, Downie SR, Kermode JA, Hardaker KM, et al. The role of the small airways in the clinical expression of asthma in adults. *J Allergy Clin Immunol* 2012;129:381-387.e1
36. Gao Y, Zhai X, Li K, Zhang H, Wang Y, Lu Y, et al. Asthma COPD overlap syndrome on CT densitometry: a distinct phenotype from COPD. *COPD* 2016;13:471-476
37. Suzuki T, Tada Y, Kawata N, Matsuura Y, Ikari J, Kasahara Y, et al. Clinical, physiological, and radiological features of asthma-chronic obstructive pulmonary disease overlap syndrome. *Int J Chron Obstruct Pulmon Dis* 2015;10:947-954
38. Kosciuch J, Krenke R, Gorska K, Zukowska M, Maskey-Warzechowska M, Chazan R. Airway dimensions in asthma and COPD in high resolution computed tomography: can we see the difference? *Respir Care* 2013;58:1335-1342
39. Kaushik SS, Cleveland ZI, Cofer GP, Metz G, Beaver D, Nouls J, et al. Diffusion-weighted hyperpolarized ^{129}Xe MRI in healthy volunteers and subjects with chronic obstructive pulmonary disease. *Magn Reson Med* 2011;65:1154-1165
40. Kirby M, Svenningsen S, Owrangi A, Wheatley A, Farag A, Ouriadov A, et al. Hyperpolarized ^{3}He and ^{129}Xe MR imaging in healthy volunteers and patients with chronic obstructive pulmonary disease. *Radiology* 2012;265:600-610
41. Jung JW, Kwon JW, Kim TW, Lee SH, Kim KM, Kang HR, et al. New insight into the assessment of asthma using xenon ventilation computed tomography. *Ann Allergy Asthma Immunol* 2013;111:90-95.e2
42. Lee CW, Seo JB, Lee Y, Chae EJ, Kim N, Lee HJ, et al. A pilot trial on pulmonary emphysema quantification and perfusion mapping in a single-step using contrast-enhanced dual-energy computed tomography. *Invest Radiol* 2012;47:92-97

 https://doi.org/10.3348/kjr.2019.0936